



Farnesol attenuates oxidative stress and liver injury and modulates fatty acid synthase and acetyl-CoA carboxylase in high cholesterol-fed rats

Mohammad H. Abukhalil^{1,2} · Omnia E. Hussein³ · May Bin-Jumah⁴ · Sultan A. M. Saghir¹ · Mousa O. Germoush⁵ · Hassan A. Elgebaly⁵ · Nermeen M. Mosa⁵ · Ismail Hamad^{6,7} · Moath M. Qarmush⁸ · Emad M. Hassanein⁹ · Emadeldin M. Kamel¹⁰ · Rene Hernandez-Bautista¹¹ · Ayman M. Mahmoud³

Received: 25 March 2020 / Accepted: 13 May 2020 / Published online: 24 May 2020
© Springer-Verlag GmbH Germany, part of Springer Nature 2020

Abstract

Dyslipidemia is a risk factor for cardiovascular disease, steatohepatitis, and progression of liver disorders. This study investigated the protective effect of farnesol (FAR), a sesquiterpene alcohol, against liver injury in high cholesterol diet (HCD)-fed rats, and its modulatory effect on fatty acid synthase (FAS) and acetyl-CoA carboxylase (ACC). HCD was supplemented for 10 weeks, and the rats were concurrently treated with FAR. Rats that received HCD exhibited significant elevation of serum cholesterol, triacylglycerols, LDL and vLDL cholesterol, CRP, and pro-inflammatory cytokines and increased values of the cardiovascular risk indices. Serum transaminases, ALP, LDH and CK-MB, and hepatic lipid peroxidation (LPO), cholesterol, and triacylglycerols were increased in HCD-fed rats. Treatment with FAR greatly ameliorated dyslipidemia and liver function, reduced inflammatory mediators, LPO, and hepatic lipid infiltration and enhanced anti-oxidant defenses. FAR suppressed hepatic FAS, ACC, and SREPB-1c mRNA abundance and FAS activity in HDC-fed rats. In addition, molecular docking simulations pinpointed the binding modes of FAR to the active pocket residues of FAS and ACC. In conclusion, FAR possesses a strong anti-hyperlipidemic/anti-hypercholesterolemic activity mediated through its ability to modulate hepatic FAS, ACC, and SREPB-1c. FAR prevented oxidative stress, inflammation, and liver injury induced by HCD. Thus, FAR may represent a promising lipid-lowering agent that can protect against dyslipidemia and its linked metabolic deregulations.

Keywords Sesquiterpenes · Hypercholesterolemia · Farnesol · Molecular docking · Oxidative stress · Steatosis

Mohammad H. Abukhalil and Omnia E. Hussein contributed as first authors.

Responsible editor: Mohamed M. Abdel-Daim

✉ Ayman M. Mahmoud
ayman.mahmoud@science.bsu.edu.eg

¹ Department of Medical Analysis, Princess Aisha Bint Al-Hussein Faculty of Nursing and Health Sciences, Al-Hussein Bin Talal University, Ma'an, Jordan

² Department of Biology, Faculty of Science, Al-Hussein Bin Talal University, Ma'an, Jordan

³ Physiology Division, Department of Zoology, Faculty of Science, Beni-Suef University, Beni Suef, Egypt

⁴ Department of Biology, College of Science, Princess Nourah bint Abdulrahman University, Riyadh, Saudi Arabia

⁵ Department of Biology, College of Science, Jouf University, Sakakah, Saudi Arabia

⁶ College of Applied Medical Sciences, Jouf University, Sakakah, Saudi Arabia

⁷ Biochemistry Department, Bahri University, Khartoum, Sudan

⁸ College of Medicine, Jouf University, Sakakah, Saudi Arabia

⁹ Department of Pharmacology and Toxicology, Faculty of Pharmacy, Al-Azhar University-Assiut Branch, Cairo, Egypt

¹⁰ Chemistry Department, Faculty of Science, Beni-Suef University, Beni Suef, Egypt

¹¹ Institute for Diabetes and Obesity, Helmholtz Center Munich, Neuherberg, Germany

Introduction

Dyslipidemia is an abnormal lipid metabolism representing the primary risk factor in the development of cardiovascular and hepatic diseases (Sozen and Ozer 2017). Lipid metabolism imbalance may result from the interaction between genetics and environmental factors, such as eating habits, especially the excessive consumption of foods rich in cholesterol and saturated fats (Bin-Jumah 2018; Ordovas 2009). Extensive evidence has demonstrated the key role of hyperlipidemia, particularly hypercholesterolemia, in the initiation of cardiovascular events in patients with cardiovascular disease (CVD) (Cífková and Krajčoviechová 2015; Han et al. 2018). In addition, it has been reported that excess accumulation of cholesterol in liver may lead to hepatotoxicity characterized by increased inflammatory cells infiltration, hepatocyte degenerative changes, and fibrosis (AlSharari et al. 2016; Farrell and Larter 2006; Muniz et al. 2019; Sozen and Ozer 2017). Furthermore, increased lipid levels in endothelial cells, hepatocytes, cardiomyocytes, leukocytes, and erythrocytes may increase reactive oxygen species (ROS) production, oxidative degradation of lipids, and membrane destabilization that eventually lead to cellular dysfunction and death (Förstermann 2008; Küçükgergin et al. 2010; Sozen and Ozer 2017). A recent study has reported that feeding a high cholesterol diet (HCD) increased serum transaminases and pro-inflammatory mediators and caused hepatic and cardiac oxidative damage in rats (Bin-Jumah 2018). Therefore, the prevention of lipid imbalance is important to prevent and treat various vascular and hepatic diseases.

Lipid accumulation in liver can occur as a result of increased synthesis and uptake of fatty acids (FAs) and/or reduced FA oxidation (Orellana-Gavaldà et al. 2011; van Herpen and Schrauwen-Hinderling 2008). Recently, fatty acid synthase (FAS) and acetyl-CoA carboxylase (ACC) have become interesting targets to assist in finding therapeutics for the treatment of obesity and hypercholesterolemia (Lu and Archer 2005). FAS, a key enzyme in the biosynthesis of FAs, catalyzes the synthesis of palmitate from acetyl-CoA, malonyl-CoA, and NADPH (Smith et al. 2003). FAS comprises seven catalytic domains (ketoacyl ACP synthase (KS), hydroxyacyl ACP dehydratase (HD), ketoacyl ACP reductase (KR), acyl transferase (AT), enoyl ACP reductase (ER), malonyl CoA-ACP transferase (MT), and thioesterase (TE)) distributed around a central acyl carrier protein (ACP) (Chirala and Wakil 2004). Each subunit is responsible for a certain function in the synthesis of palmitate. The TE domain was identified as the main factor controlling the last step of FAs synthesis, particularly the release of palmitate by the hydrolysis of thioester linkage in palmitoyl-S-ACP (Chirala and Wakil 2004). The KS domain is responsible for the production of various-length FAs (Witkowski et al. 2002). ACC is a biotin-dependent enzyme catalyzing the production of malonyl-

CoA from acetyl-CoA. This ACC-catalyzed reaction is an important step in modulating both the biosynthesis and oxidation of FAs (Xiang et al. 2009). ACC consists of biotin carboxylase (BC), biotin carboxy carrier protein (BCCP), and carboxy transferase (CT) domains (Corbett et al. 2010). The binding modes of the active inhibitors with FAS and ACC are still a matter of debate. The lack of this knowledge has increased the curiosity toward better understanding of the interactions of these enzymes with reactive drugs.

The use of plants and their products in the treatment of hyperlipidemia is an ongoing approach worldwide. Indeed, natural compounds with anti-oxidant and lipid-lowering actions may confer beneficial effects against the serious pathological consequences of cholesterol accumulation in certain tissues, such as liver and heart. Farnesol (FAR; 3,7,11-trimethyldodeca-2,6,10-trien-1-ol) is a sesquiterpene alcohol widely distributed in fruits, vegetables, essential oils, and herbs. Peaches, tomatoes, corn, chamomile, lemon grass, and citronella and ambrette seeds oils are among the sources of FAR (Goto et al. 2011; Jung et al. 2018; Tatman and Mo 2002). Numerous biological activities of FAR, including anti-oxidant, anti-inflammatory, anti-obesity, hepatoprotective and cardioprotective effects have been documented (Jung et al. 2018; Kim et al. 2017; Lateef et al. 2013). FAR protected the lungs against cigarette smoke-induced injury by mitigating inflammation and oxidative stress in rats (Santhanasabapathy et al. 2015). Besides, FAR was shown to ameliorate acrylamide-induced inflammation and neurotoxicity in mice by suppressing inflammatory mediators (Qamar and Sultana 2008). FAR has also prevented ischemia/reperfusion (I/R) injury by increasing protein geranylgeranylation and enhancing anti-oxidant activity in cardiomyocytes (Szűcs et al. 2013) and protected against calcium overload-induced arrhythmia through decreasing ROS generation in rats (de Souza et al. 2019). Moreover, FAR has been shown to modulate lipid profile by reversing the aberrated low-density lipoprotein (LDL) cholesterol/high-density lipoprotein (HDL) cholesterol and HDL cholesterol/total cholesterol ratios in asthmatic mice (Ku and Lin 2015). Another study showed that FAR reduced serum triglyceride (TG) and enhanced metabolic abnormalities by regulating PPAR α in hepatocytes (Goto et al. 2011). FAR has also been shown to suppress 3-hydroxy-3-methylglutaryl coenzyme A (HMG-CoA) reductase, a key enzyme in cholesterol synthesis (Meigs et al. 1996) and inhibit phosphatidylcholine synthesis human leukemic CEM-C1 cell line (Voziyan et al. 1993) and de novo synthesis of TG in hepatocytes (Hiyoshi et al. 2003). However, the exact anti-hypercholesterolemic mechanism of FAR remains to be further elucidated. Therefore, this study was conducted to explore the mechanism by which FAR may exert beneficial effects on lipid metabolism through studying its effect on hepatic LDL receptor (LDLR), FAS, ACC, and sterol regulatory element-binding protein-1c (SREPB-1c) in HCD-fed rats.

We have also investigated the binding interactions between FAR and ACC and FAS by molecular docking simulations. Furthermore, the protective effect of FAR against hypercholesterolemia-induced oxidative stress and inflammation in the liver of rats was assessed.

Materials and methods

Experimental animals and treatments

Seven-week-old male albino Wistar rats of 140–160 g body weight obtained from VACSERA (Giza, Egypt) were included in this study. The animals were housed under standard conditions (temperature, 23 ± 2 °C) and a 12-h light/dark cycle) and acclimatized for 1 week before starting the experiment with free access to food and water.

Thirty rats were randomly allocated into five groups ($n = 6$) as follows:

- Group I (Control): received normal diet for 10 weeks.
- Groups II (HCD): received HCD (normal diet supplemented with 2% cholesterol) for 10 weeks (Bin-Jumah 2018).
- Group III (HCD + 5 mg kg⁻¹ FAR): received HCD and 5 mg kg⁻¹ day⁻¹ FAR (Sigma, USA) for 10 weeks.
- Group IV (HCD + 10 mg kg⁻¹ FAR): received HCD and 10 mg kg⁻¹ day⁻¹ FAR for 10 weeks.
- Group V (HCD + SIM): received HCD and 10 mg kg⁻¹ day⁻¹ simvastatin (SIM) (Al-Rasheed et al. 2015) for 10 weeks.

FAR was dissolved in corn oil and the doses were selected according to previous studies showing its anti-oxidant and anti-inflammatory activities in different experimental models (Kim et al. 2017; Lateef et al. 2013; Ong et al. 2006). FAR has been supplemented at doses ranging from 5 to 250 mg kg⁻¹ body weight. The 5-mg kg⁻¹ dose exerted an anti-obesity effect in high fat diet (HFD)-fed mice (Kim et al. 2017) and hence selected along with a higher dose in this study. FAR and SIM were supplemented orally, and groups I and II received the vehicle for 10 weeks.

Collection and preparation of samples

Twenty-four hours after the last treatment, overnight fasted rats were killed under thiopental (Eipico, Egypt) anesthesia, and blood was collected via cardiac puncture. Serum was prepared and used for the analysis of cholesterol, TG, HDL cholesterol, alkaline phosphatase (ALP), lactate dehydrogenase (LDH), alanine aminotransferase (ALT), aspartate aminotransferase (AST), and creatine kinase-MB (CK-MB), C-reactive protein (CRP), tumor necrosis factor (TNF)- α ,

interleukin (IL)-6, and IL-1 β . The rats were killed, dissected, and liver excised. Small pieces from the liver were fixed in 10% neutral buffered formalin for histological investigation, and other pieces were frozen at -80 °C. Other samples were homogenized (10%, w/v) in cold PBS, centrifuged, and the clear homogenate was used for the assessment of different biochemical parameters.

Biochemical assays

Determination of lipids and cardiovascular risk indices

Total cholesterol, TG, and HDL cholesterol in serum were determined using colorimetric assay kits (Spinreact, Spain) following the provided instructions. LDL- and vLDL cholesterol, cardiovascular risk indices (Ross 1992), and anti-atherogenic index (AAI) (Guido and Joseph 1992) were calculated using the formulas:

$$\text{vLDL cholesterol} = \text{triglycerides}/5$$

$$\text{LDL cholesterol} = \text{total cholesterol} - (\text{HDL cholesterol} + \text{vLDL cholesterol})$$

$$\text{Cardiovascular risk index 1} = \text{total cholesterol}/\text{HDL cholesterol}$$

$$\text{Cardiovascular risk index 2} = \text{LDL cholesterol}/\text{HDL cholesterol}$$

$$\text{AAI} = \text{HDL cholesterol} \times 100 / (\text{total cholesterol} - \text{HDL cholesterol})$$

To determine hepatic cholesterol and TG levels, total lipids were extracted according to Folch et al. (1957). Cholesterol and TG were measured using Spinreact (Spain) kits.

Determination of liver and heart function markers, CRP, and pro-inflammatory cytokines

Serum ALT, AST, ALP, LDH, and CK-MB were estimated using kits supplied by Spinreact (Spain). Serum levels of CRP, TNF- α , IL-1 β , and IL-6 were measured employing ELISA kits (R&D Systems, USA). All measurements were conducted following the manufactures' guidelines.

Assay of lipid peroxidation, anti-oxidant defenses, and FAS activity

Malondialdehyde (MDA), a marker of lipid peroxidation (LPO) (Ohkawa et al. 1979), reduced glutathione (GSH) (Beutler et al. 1963), SOD (Marklund and Marklund 1974), and CAT (Cohen et al. 1970) were assayed in the supernatant of homogenized liver samples. FAS activity was assayed following the method described by Goodridge (1972). The assay depends on following the decrease in absorbance resulting from NADPH oxidation at 340 nm following the addition of malonyl-CoA. FAS activity was expressed as nanomole-reduced NADPH per minute per milligram of protein. Total protein content was determined using Bradford (1976) reagent.

Histological examination of liver sections

Liver specimens were obtained and washed in ice-cold PBS and immediately fixed in 10% formalin for 24 h at 4 °C. After fixation, the specimens were dehydrated and processed for embedding in paraffin wax. Five-micrometer sections were obtained using microtomy and then stained with hematoxylin and eosin (H&E) for microscopic examination.

Gene expression analysis

The mRNA expression levels of LDLR, FAS, ACC, and SREPB-1c were quantified using qRT-PCR. Briefly, total RNA was extracted from frozen tissue samples using TRIzol (Invitrogen, USA). RNA samples were treated with RNase-free DNase and quantified at 260 nm. The quality of the RNA samples was examined using formaldehyde-agarose electrophoresis, and the purity was determined using OD260/OD280 nm absorption ratio ≥ 1.8 . Next, 2 μg RNA was reverse transcribed, and the obtained cDNA was amplified using QuantiFast SYBR Green RT-PCR kit (Qiagen, Germany) and primers in Table 1. The obtained data were analyzed using the $2^{-\Delta\Delta\text{Ct}}$ method (Livak and Schmittgen 2001) and normalized to β -actin.

Molecular docking

The initial 3D structure of FAR was constructed using gaussview 6. The geometry of FAR was optimized at the B3LYP level of theory with the 6-311G (d, p) basis set (Becke 1993). The output was converted to .pdb 3D structures using UCSF Chimera (Pettersen et al. 2004). Autodock Tools (ADT) v1.5.6 and AutoDock Vina software packages were employed for molecular docking simulations (Trott and Olson 2010). FAR was optimized for docking by using ADT. To visualize the binding mode FAR-protein complexes, the PyMOL v2.3.2 program was employed. X-ray crystal structure of the ACC used for docking was obtained from the protein data bank (PDB ID: 3TV5). Human FAS domains were utilized for docking, namely KS (PDB ID:3HHD) and TE (PDB ID: 1XKT). Macromolecules were viewed and

isolated from ligands, solvent, and nonstandard residues by using UCSF Chimera. Separated proteins were set for docking by optimization using ADT. The optimization includes addition of polar hydrogens and adjusting the grid box according to the suitable configuration of the active site residues (Cheng et al. 2008). The size of grid box for ACC was set at $60 \times 60 \times 75$ (x,y,z). The KS and TE of the grid boxes were placed at $60 \times 60 \times 60$ (x,y,z) and $50 \times 50 \times 50$ (x,y,z), respectively.

Statistical analysis

The obtained results were represented as mean \pm standard error of the mean (SEM). All statistical comparisons were determined by one-way ANOVA and Tukey’s test using GraphPad Prism 7 (GraphPad Software, La Jolla, CA, USA). Data of the body weight changes were analyzed by two-way ANOVA and Tukey’s test. A *P* value < 0.05 was considered significant.

Results

Effect of FAR on body weight of HCD-fed rats

Body weight was steadily increased in all groups as represented in Fig. 1a. At weeks 8–10, HCD-fed rats exhibited a significant increase in body weight ($P < 0.001$) when compared with the control rats (Fig. 1b). Treatment with FAR and SIM prevented the HCD-induced significant increase in body weight ($P < 0.001$).

FAR attenuates dyslipidemia in HCD-fed rats

To assess the anti-dyslipidemia effect of FAR, serum lipids were measured. HCD supplementation caused a significant increase in serum TG (Fig. 2a), total cholesterol (Fig. 2b), LDL cholesterol (Fig. 2c), and vLDL cholesterol (Fig. 2d), while it did not significantly alter serum HDL cholesterol levels (Fig. 2e). Treatment with FAR (5 and 10 mg kg^{-1}) or SIM significantly reinstated HCD-induced increased serum lipids near to the normal levels. HCD-fed rats received FAR

Table 1 Primers used for qRT-PCR

Gene	Accession number	Forward primer (5'-3')	Reverse primer (5'-3')
<i>FAS</i>	NM_017332	GCCTAACACCTCTGTGCAGT	GGCAATACCCGTTCCCTGAA
<i>ACC</i>	NM_022193	TTGGTGCTTATATTGTGGAT	ATGTGCCGAGGATTGATGG
<i>LDLR</i>	NM_175762	CAGCTCTGTGTGAACCTGGA	TTCTTCAGGTTGGGGATCAG
<i>SREBP1c</i>	NM_001276707	CATCAACAACCAAGACAGTG	GAAGCAGGAGAAGAGAAGC
<i>β-Actin</i>	NM_031144	AGGAGTACGATGAGTCCGGC	CGCAGCTCAGTAAC AGTCCG

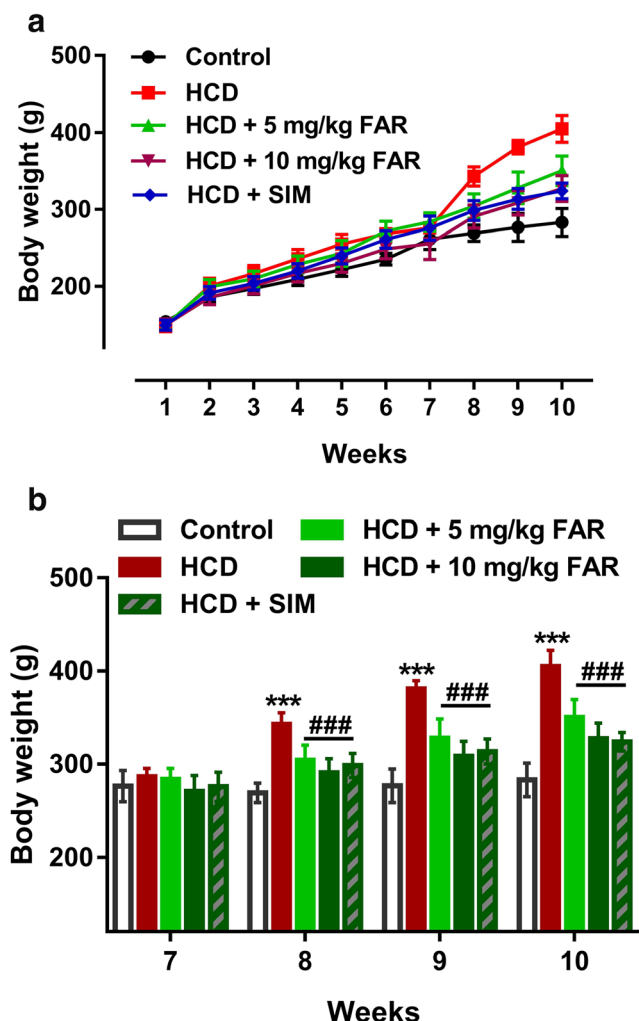


Fig. 1 Body weight changes in control and HCD-fed rats. FAR and SIM prevented the significant increase in body weight of HCD-fed rats at weeks 8–10. Data are mean \pm SEM, $n = 6$. *** $P < 0.001$ versus control; ### $P < 0.001$ FAR (5 and 10 mg) and SIM versus HCD

or SIM showed non-significant changes in serum HDL cholesterol.

HCD-supplemented rats exhibited a significant elevation in the values of total cholesterol/HDL cholesterol (Fig. 3a), and LDL cholesterol/HDL cholesterol ratios (Fig. 3b). On the other hand, there was a significant reduction in AAI in HCD-fed rats (Fig. 3c). Remarkably, treatment with FAR or SIM alleviated these cardiovascular risk indices.

FAR prevents hepatic lipid accumulation and tissue injury in HCD-fed rats

Liver cholesterol and TG content, and serum transaminases, ALP and LDH were determined and a histological investigation was carried out to investigate the ameliorative effect of FAR on HCD-induced liver injury. HCD feeding for 10 weeks resulted in increased hepatic cholesterol (Fig. 4a) and TG (Fig. 4b) significantly ($P < 0.001$) when compared with the control

rats. Treatment with FAR (5 and 10 mg kg^{-1}) and SIM decreased liver cholesterol and TG levels in HCD-fed rats. In addition, histological examination revealed fatty infiltrations and hepatic vacuolations in the liver of HCD-fed rats (Fig. 5b) when compared with the control rats which showed normal structure of the hepatic lobules, hepatocytes and sinusoids (Fig. 5a). Rats received 5 and 10 mg kg^{-1} FAR (Fig. 5c, d, respectively) and SIM (Fig. 5e) showed remarkable reduction in the infiltration of fats with only mild vacuolations were observed. Furthermore, there was a significant ($P < 0.001$) increase in serum ALT, AST, ALP, and LDH in HCD-fed rats (Fig. 6a–d), indicating hepatic injury. All these changes were significantly ameliorated in HCD-fed rats treated with FAR or SIM. Serum CK-MB was determined to evaluate the cardioprotective efficacy of FAR. While the HCD-fed rats exhibited a significant elevation in serum CK-MB, FAR-treated groups showed a significant reduction (Fig. 6e).

FAR diminishes hepatic LPO and enhances anti-oxidants in HCD-fed rats

Since hypercholesterolemia may induce oxidative stress, this study also evaluated the effect of FAR on LPO and anti-oxidant defenses in the liver of HCD-fed rats. There was a significant increase in hepatic MDA (Fig. 7a; $P < 0.001$), and decreased GSH (Fig. 7b; $P < 0.001$), SOD (Fig. 7c; $P < 0.001$), and CAT (Fig. 7d; $P < 0.01$) in rats supplemented a HCD for 10 weeks. Remarkably, treatment with FAR (5 and 10 mg kg^{-1}) or SIM attenuated oxidative stress in the liver as evidenced by decreased LPO and increased GSH and anti-oxidant enzymes.

FAR suppresses inflammation in HCD-fed rats

To evaluate the possible role of inflammation in HCD-induced liver injury and the protective effects of FAR, serum CRP and pro-inflammatory cytokines were assayed. There was a significant ($P < 0.001$) increase in CRP (Fig. 8a), TNF- α (Fig. 8b), IL-6 (Fig. 8c), and IL-1 β (Fig. 8d) levels in rats that received HCD for 10 weeks when compared with the control group. Nevertheless, treatment with FAR or SIM significantly ($P < 0.001$) ameliorated serum levels of CRP and cytokines.

FAR modulates hepatic LDLR, SREBP-1c, FAS, and ACC in HCD-fed rats

To understand the anti-dyslipidemia activity of FAR in HCD-fed rats, we evaluated its effect on key factors involved in de novo lipogenesis, namely SREBP-1c, FAS, and ACC, as well as LDLR. While LDLR (Fig. 9a) showed non-significant changes upon HCD feeding, SREBP-1c (Fig. 9b), FAS (Fig. 9c), and ACC (Fig. 9e) mRNA abundance were significantly ($P < 0.001$) increased in the liver of HCD-fed rats. Moreover, hepatic FAS activity was significantly increased in HCD-fed

Fig. 2 FAR attenuates dyslipidemia in HCD-fed rats. FAR and SIM reduced serum TG (a), and total- (b), LDL- (c), and vLDL cholesterol (d), but did not increase HDL cholesterol (e) significantly in HCD-fed rats. Data are mean ± SEM, *n* = 6. ****P* < 0.001 versus control; ###*P* < 0.001 versus HCD

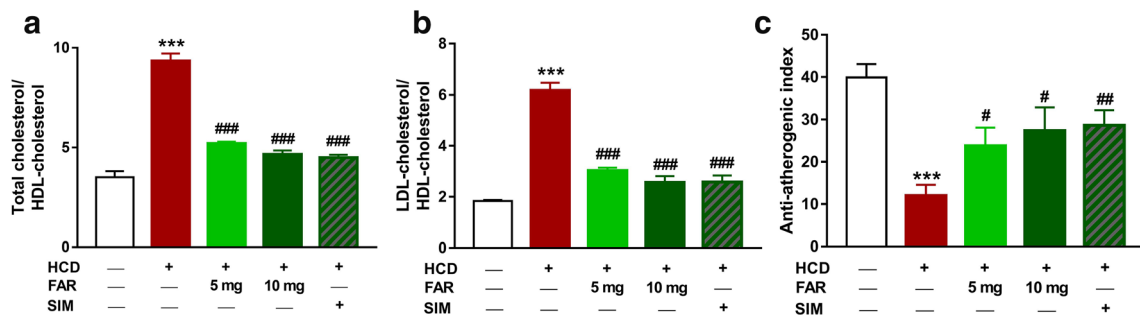
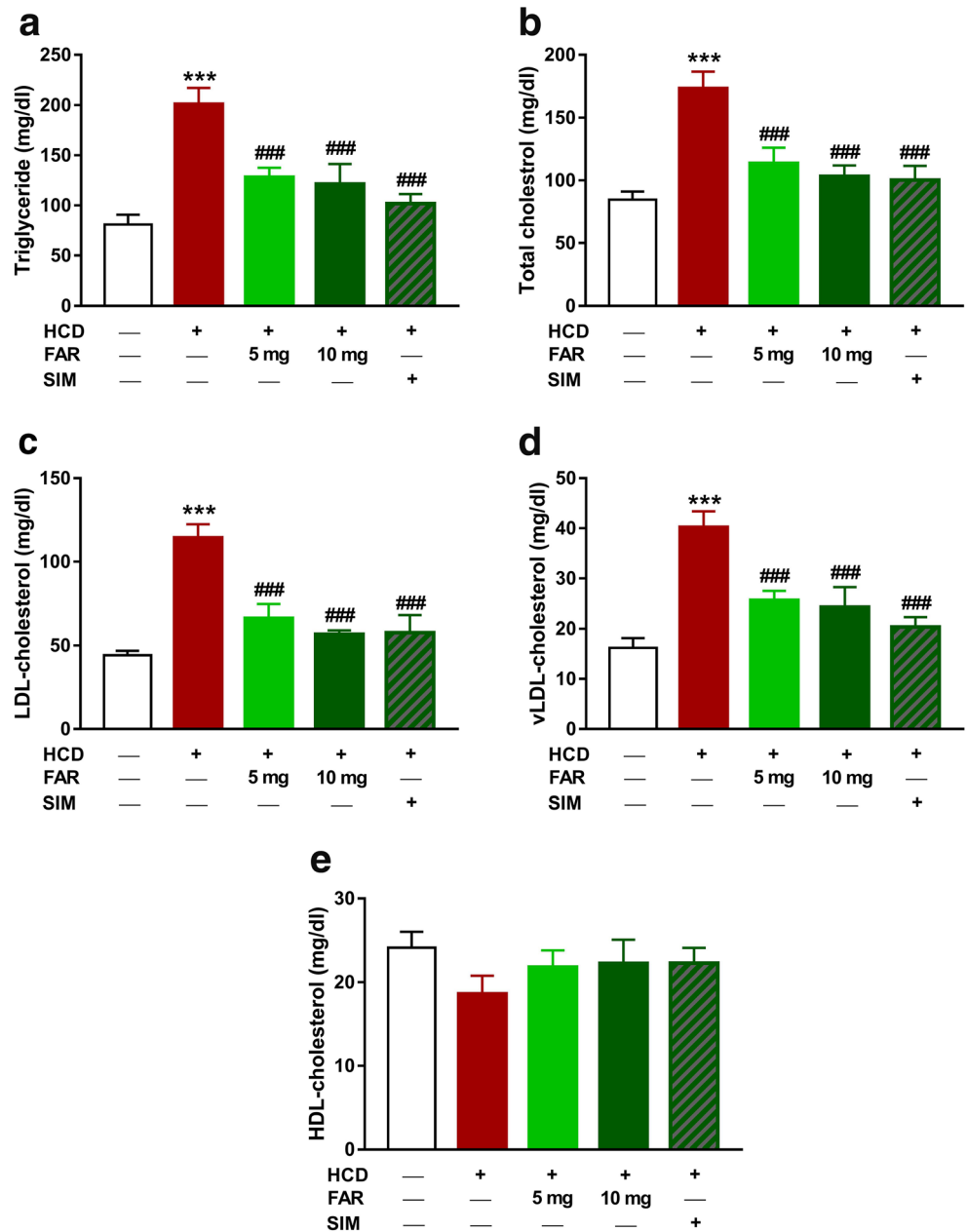
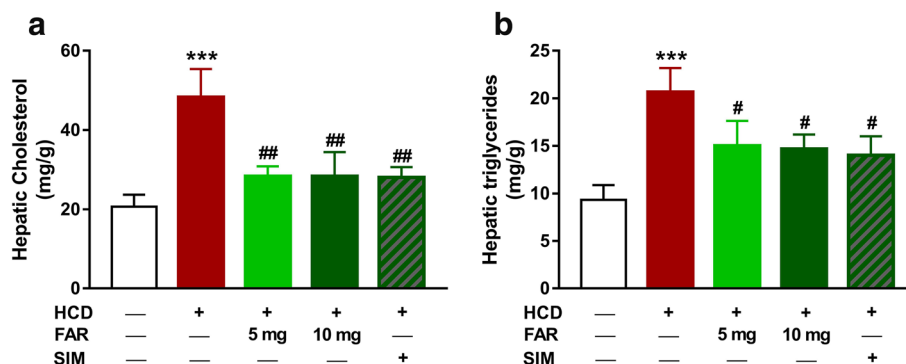


Fig. 3 FAR prevents atherogenesis in HCD-fed rats. FAR and SIM decreased cardiovascular risk indices (a, b) and increased anti-atherogenic index (c). Data are mean ± SEM, *n* = 6. ****P* < 0.001 versus control; #*P* < 0.05, ##*P* < 0.01, and ###*P* < 0.001 versus HCD

Fig. 4 FAR attenuates lipid accumulation in liver of HCD-fed rats. FAR and SIM decreased hepatic cholesterol (a) and triglycerides (b) in HFD-fed rats. Data are mean \pm SEM, $n = 6$. *** $P < 0.001$ versus control and # $P < 0.05$ and ## $P < 0.01$ versus HCD



rats (Fig. 9d) as compared with the control rats. Interestingly, FAR and SIM significantly restored hepatic mRNA levels of LDLR, SREBP-1c, FAS, and ACC, as well as FAS activity.

To further explore the modulatory effect of FAR on FAS and ACC, we performed molecular docking analysis to figure out their binding modes. FAR was shown to dock into the

determined active site of TE domain of FAS, as represented in Fig. 10a, b. A detailed investigation of the binding site indicated that FAR forms four hydrogen bonds with the residues Ser2308, Asp2338, His2481, and Arg2482 in FAS. In addition, FAR was placed in the binding cavity encased by the hydrophobic residues Leu2222, Ile2250, Glu2251, Phe2370,

Fig. 5 Photomicrographs of liver sections of a control rats showing normal structure of hepatocytes and central vein and no alterations, b HCD-fed rats showing vacuolation of round border and clear vacuoles consistent with fatty changes (arrows), c–e HCD-fed rats treated with 5 mg kg⁻¹ FAR (c), 10 mg kg⁻¹ FAR (d), and SIM (e) showing remarkable improvement of liver architecture with slight vacuolations. (H&E, $\times 400$; scale bar, 50 μ m)

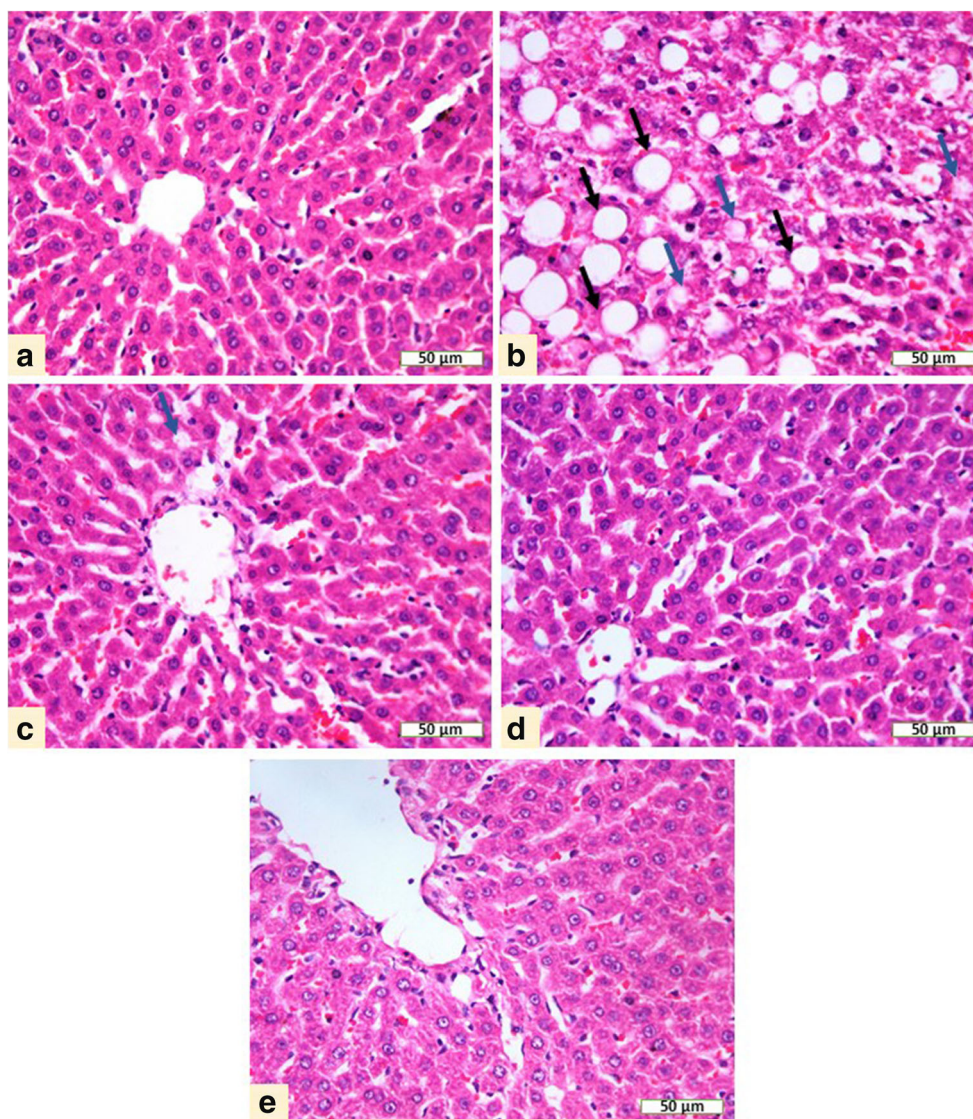
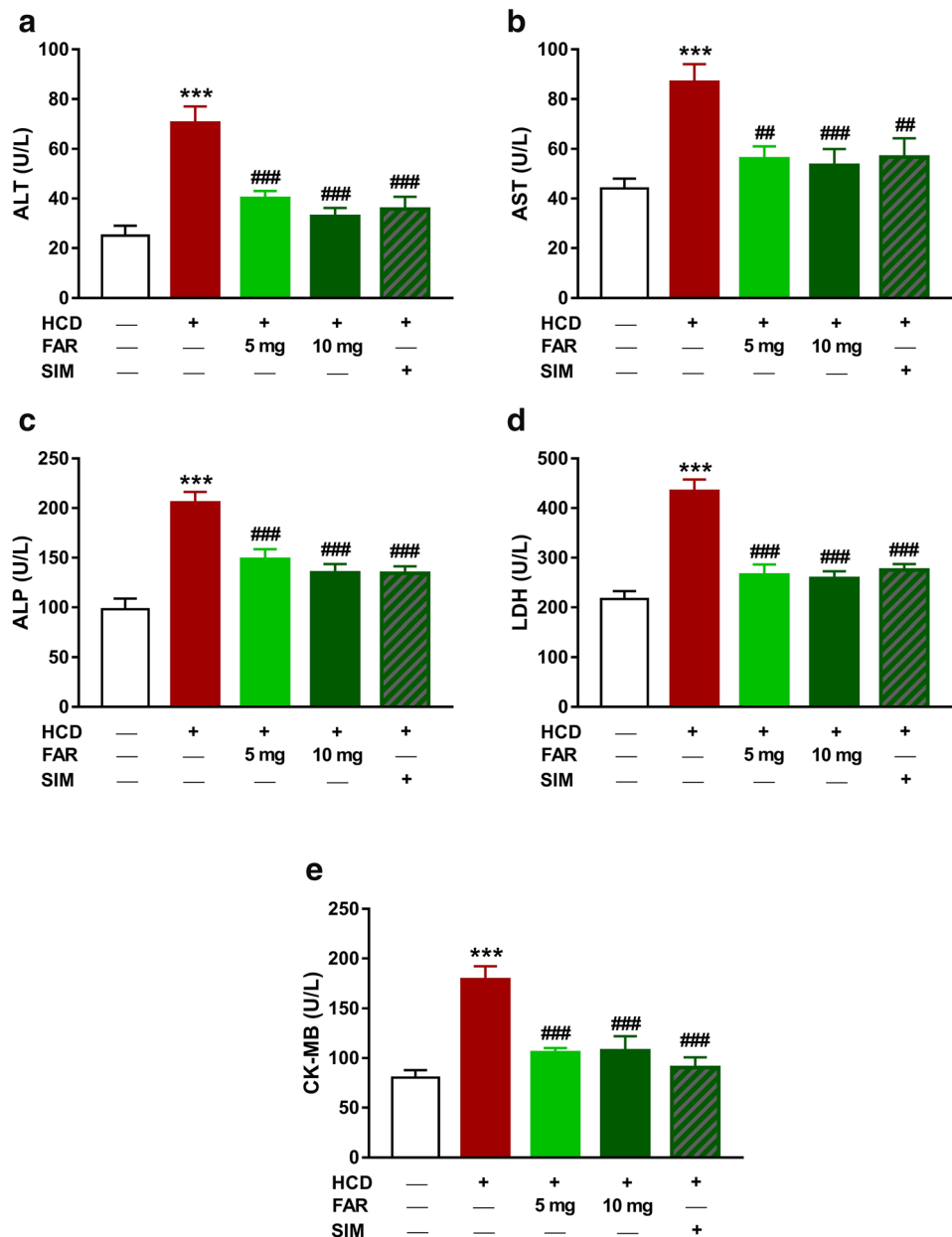


Fig. 6 FAR prevents liver and heart injury in HCD-fed rats. FAR and SIM reduced serum ALT (a), AST (b), ALP (c), LDH (d), and CK-MB (e) significantly in HCD-fed rats. Data are mean ± SEM, *n* = 6. ****P* < 0.001 versus control; ##*P* < 0.01 and ###*P* < 0.001 versus HCD



Phe2371 Gln2374, and Phe2423. The binding affinity was $-5.2 \text{ kcal mol}^{-1}$, indicating the formation of a stable FAR-FAS/TE domain complex. These polar and hydrophobic interactions reflect the stability of FAR-binding pattern with TE. Three phenylalanine residues (Phe2370, Phe2371, and Phe2432) were closely detected in the binding site of FAR-FAS/TE domain complex. This information is of particular interest, since it shed the light on the probability for these residues to exhibit a thermodynamically favorable π - π interactions. These interactions are likely to contribute in the binding mechanism of FAR with FAS.

The *in silico* model for the interaction of KS domain of FAS with FAR was developed by our molecular docking studies. FAR was located in the binding site surrounded by

residues Cys161, Met205, Tyr222, Pro264, His293, Thr295, Thr297, Gln303, His331, Phe393, Gly394, and Phe395. Also, FAR formed two hydrogen bonds with residues Gln269 and Gly300, as shown in Fig. 10c, d. A lower binding energy was obtained for this complex than its TE domain counterpart ($-6.7 \text{ kcal mol}^{-1}$). Two phenylalanine residues in the hydrophobic pocket make this interaction more susceptible to stabilization by π - π interaction effects.

The binding interaction between FAR and human ACC is represented in Fig. 10e, f. Three polar bonds were detected in the FAR-ACC complex with residues Ser1808 and Arg1883, and occupied hydrophobic pocket comprises the residues Gln1522, Asn1525, Phe1526, Pro1574, Glu1575, Glu1805, Tyr 1809, Leu1821, Lys1863, and Gly1864. The complex

Fig. 7 FAR diminishes hepatic LPO and enhances anti-oxidants in HCD-fed rats. FAR and SIM reduced MDA (a) and increased GSH (b), SOD (c), and CAT (d) in liver of HCD-fed rats. Data are mean \pm SEM, $n = 6$. $^{***}P < 0.01$ and $^{***}P < 0.001$ versus control; $^{\#}P < 0.05$, $^{\#\#}P < 0.01$, and $^{\#\#\#}P < 0.001$ versus HCD

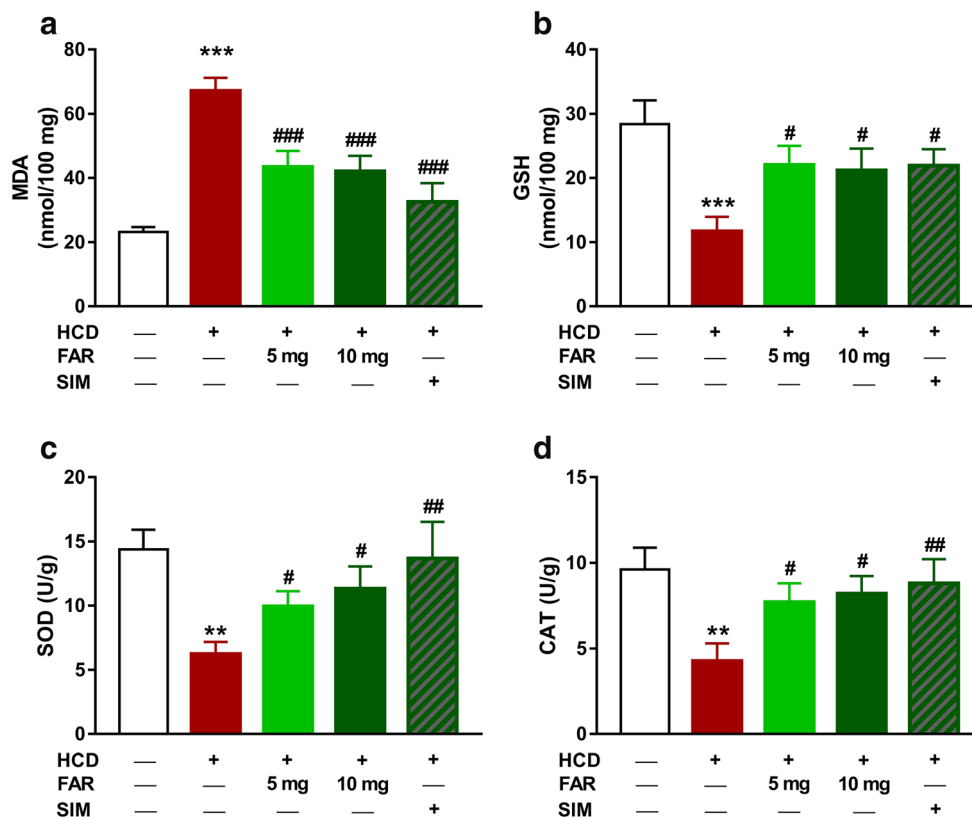


Fig. 8 FAR suppresses inflammation in HCD-fed rats. FAR and SIM decreased serum CRP (a), TNF- α (b), IL-6 (c), and IL-1 β (d) in HCD-fed rats. Data are mean \pm SEM, $n = 6$. $^{***}P < 0.001$ versus control; $^{\#}P < 0.05$, $^{\#\#}P < 0.01$, and $^{\#\#\#}P < 0.001$ versus HCD

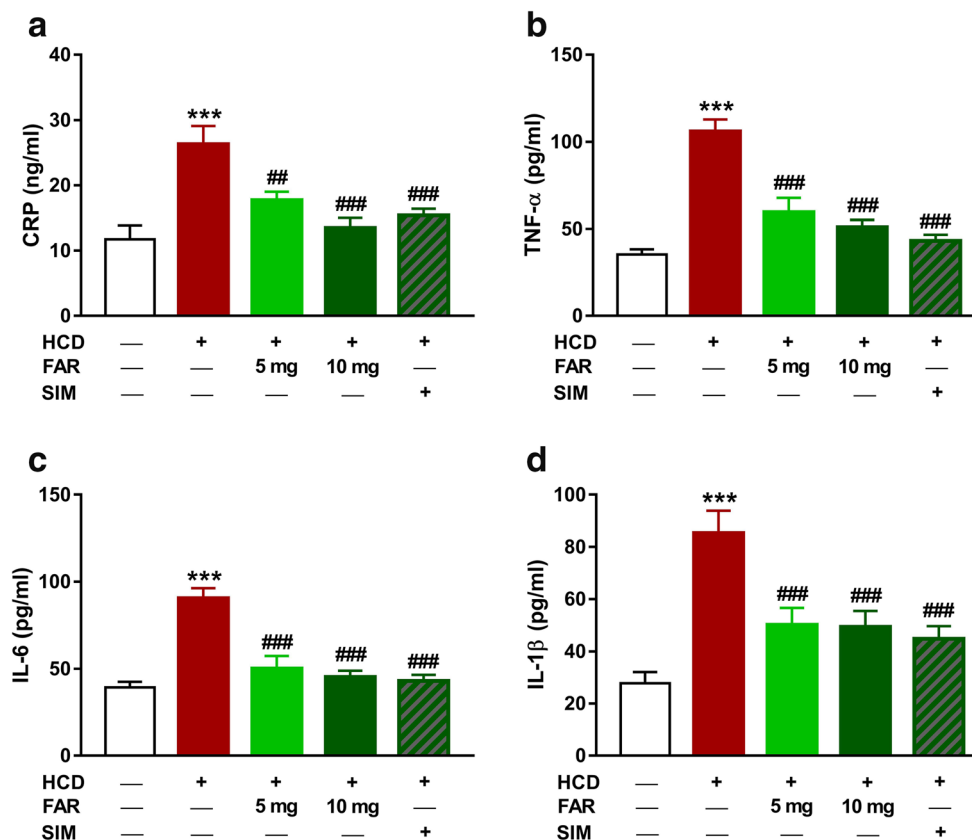
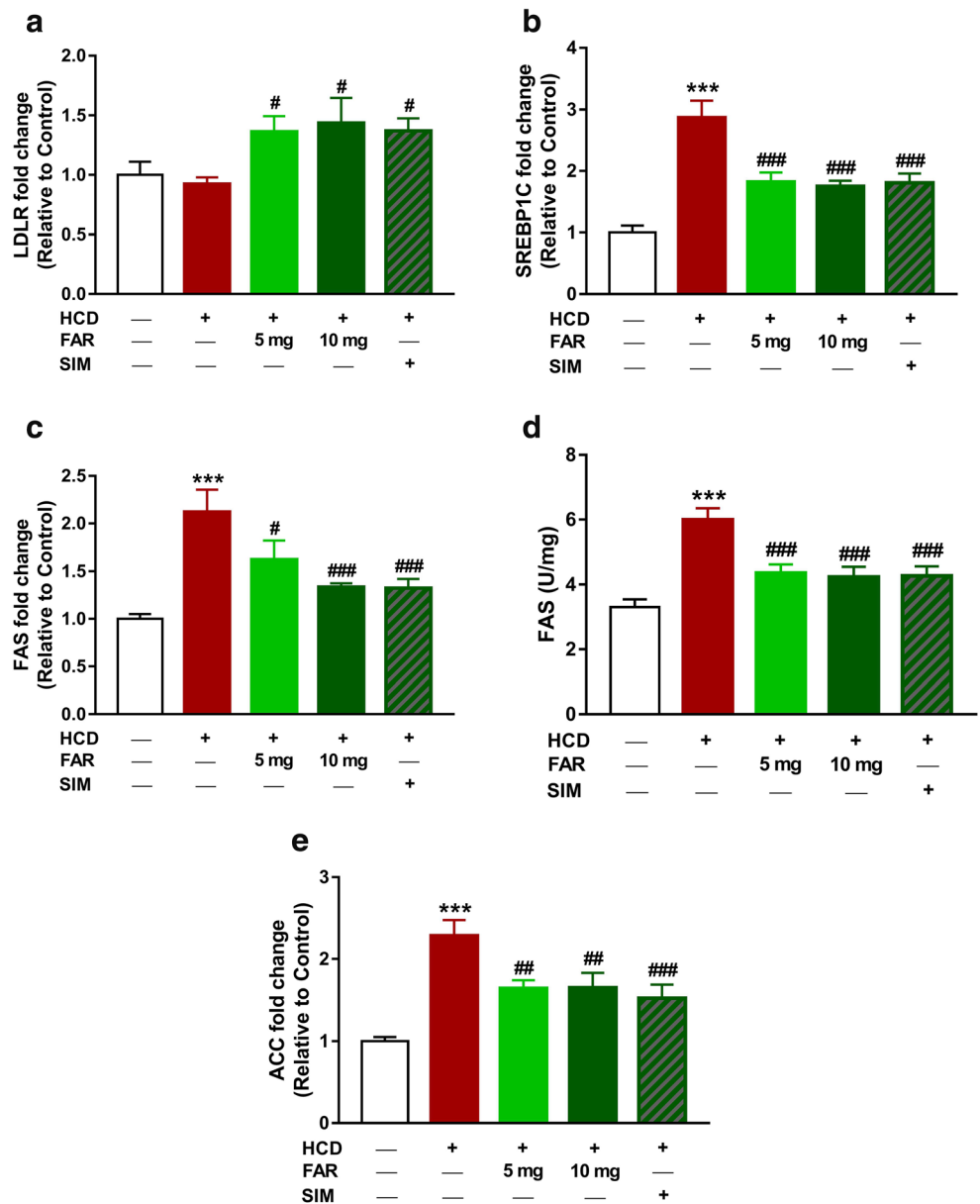


Fig. 9 FAR modulates hepatic LDLR, SREBP-1c, FAS, and ACC in HCD-fed rats. FAR and SIM increased hepatic LDLR (a) and decreased SREBP-1c (b), FAS (c, d), and ACC (e) mRNA abundance and FAS activity in HCD-fed rats. Data are mean ± SEM, *n* = 6. ****P* < 0.001 versus control; #*P* < 0.05, ###*P* < 0.01, and *P* < 0.001 versus HCD



formed is stable and the lowest binding energy was $-5.5 \text{ kcal mol}^{-1}$. The estimated binding pocket in this complex showed one phenylalanine and one tyrosine residues, namely Phe1526 and Tyr1809. These residues are capable of making π - π interactions that could potentially show thermodynamically favorable interactions with the pi bonds of the inhibitor. Figure 8e shows the structure of the potential depth in the binding cavity of FAR-ACC-binding pocket. This figure implies that FAR is located mainly inside the binding pocket of ACC.

Discussion

Hypercholesterolemia is a well-acknowledged causative risk factor for the development of CVD and liver injury (Sozen

and Ozer 2017). Thus, hypocholesterolemic strategies could be effective in preventing metabolic disorders associated with dyslipidemia. Herein, we investigated the potential of FAR to prevent liver injury in HCD-fed rats, pointing to its ability to suppress oxidative stress, inflammation and lipogenic factors. Our results showed that FAR effectively attenuated dyslipidemia, oxidative stress and liver injury, and modulated SREBP-1c, FAS, and ACC.

HCD feeding has been reported to establish an experimental model mimicking hypercholesterolemia pathophysiology in human (Shi et al. 2019). Consistent with several previous studies (AlSharari et al. 2016; Bin-Jumah 2018; Shi et al. 2019), HCD caused dyslipidemia manifested by increased serum cholesterol, TG, and LDL and vLDL. Hypercholesterolemia can lead to hepatic lipid accumulation resulting in chronic

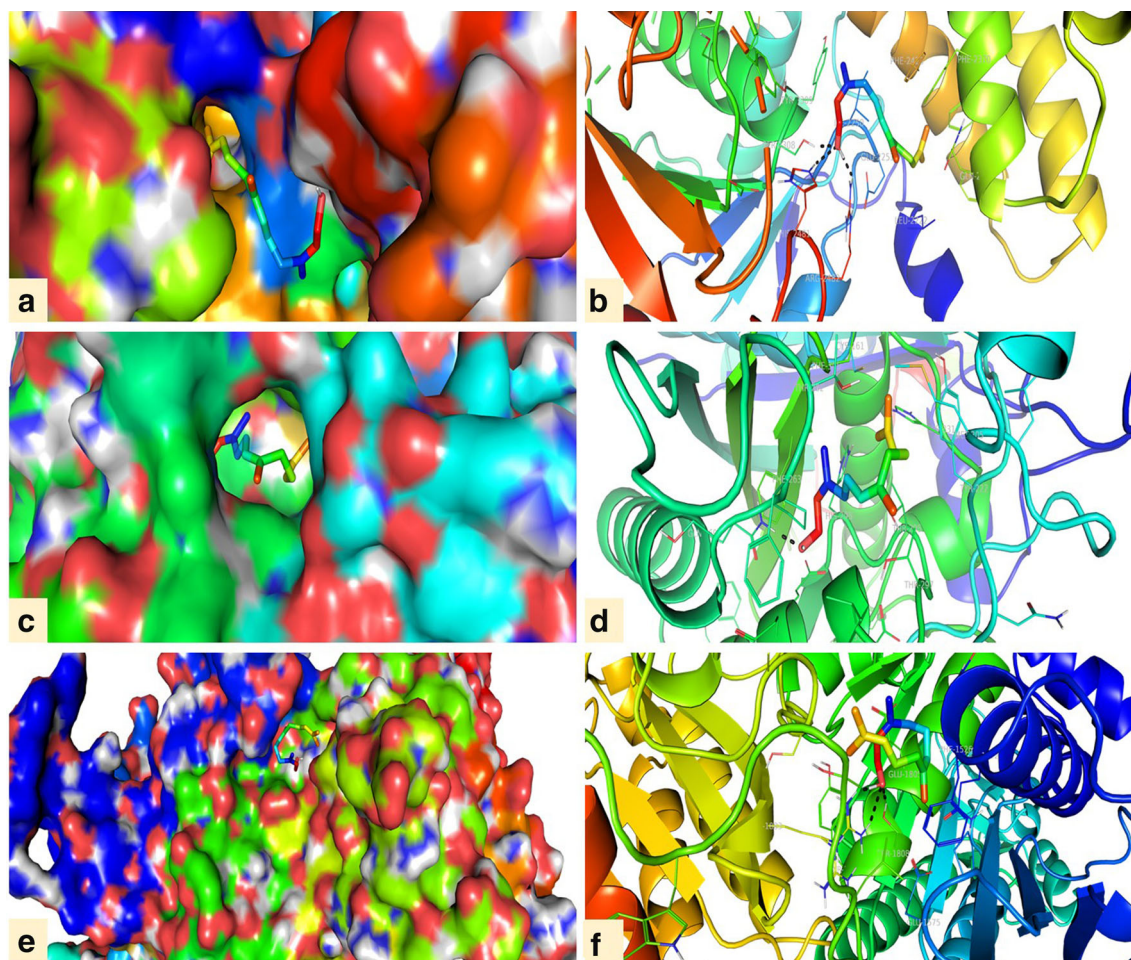


Fig. 10 Docking models of FAR with **a** FAS/TE, **b** FAS/KS, and **c** ACC

inflammation, degenerative changes, hepatotoxicity, fibrosis, and liver failure (AlSharari et al. 2016; Farrell and Larter 2006; Muniz et al. 2019; Sozen and Ozer 2017). Accordingly, cholesterol and TG were increased in the liver of HCD-fed rats and histological examination revealed massive lipid infiltration. Increased accumulation of lipids in the liver can impact its ability to metabolize lipids, resulting in dyslipidemia (Arvind et al. 2000). HCD-induced liver injury has been further confirmed by elevated serum transaminases, ALP and LDH. These enzymes are the most frequently used indicators for the assessment of liver injury and are considered valuable markers of degenerative and necrotic changes in hepatocytes (McGill 2016). Here, treatment with FAR and SIM reduced serum lipids and hepatic cholesterol and TG contents in HCD-fed rats. In addition, the histopathological findings revealed a remarkable reduction in hepatic lipid infiltration following treatment with FAR or SIM. FAR has also reduced serum ALT, AST, ALP, and LDH in HCD-fed rats, demonstrating a potent hepatoprotective activity. In this context, FAR showed a protective effect against cyclophosphamide (CP) hepatotoxicity in mice (Araghi et al. 2018). Treatment with FAR reduced serum ALT and AST and preserved the normal architectural integrity of liver in CP-

intoxicated mice (Araghi et al. 2018). Hypercholesterolemia may also impact the myocardium resulting in contractile dysfunction, I/R injury, and diminished stress adaptation (Csonka et al. 2016; Huang et al. 2004; Osipov et al. 2009). Therefore, lipid-lowering strategies might help in counteracting the negative impact of hypercholesterolemia on the heart. The present study demonstrated that HCD-fed rats showed significantly elevated cardiovascular risk indices and reduced AAI, coupled with increased serum levels of CK-MB, a key biomarker of heart function, which were remarkably attenuated by FAR treatment. Thus, these findings indicate that the anti-hyperlipidemic effect of FAR mediated its cardioprotective action.

Given that cholesterol-enriched diet was reported to induce oxidative stress in various tissues (Abbas and Sakr 2013; Bin-Jumah 2018; Kocsis et al. 2009), we assumed that the antioxidant activity of FAR plays a role in its hepatoprotective efficacy. Hypercholesterolemia has been implicated in oxidative modification of LDL, protein glycation, and glucose autooxidation (Singh et al. 2017; Yang et al. 2008). Besides, high cholesterol levels can lead to increased cholesterol pool, which results in changes in cell membrane physical properties, facilitating the leakage of ROS from the mitochondrial

electron system or the activation of NADPH oxidase and xanthine oxidase, eventually culminating in LPO and protein oxidation (Singh et al. 2017; Varga et al. 2013). Here, HCD-fed rats showed an increase in MDA coupled with decreased GSH and activity of the anti-oxidant enzymes. LPO alters fluidity and permeability of cell membranes and inactivate membrane-bound receptors and enzymes, leading to destruction of the membrane (Singh et al. 2017; Smathers et al. 2011). Moreover, increased ROS production can promote oxidation of the anti-oxidant enzymes and therefore abolish the cellular anti-oxidant capacity (Smathers et al. 2011). Therefore, attenuation of hypercholesterolemia-induced oxidative stress could represent an effective strategy to prevent or treat metabolic abnormalities in hyperlipidemic subjects. In the present study, FAR diminished LPO and boosted GSH and anti-oxidant enzymes in the liver of HCD-fed rats. Consistently, FAR prevented CP-induced oxidative damage in mice liver (Araghi et al. 2018) and protected against cigarette smoke-induced oxidative stress in rats prostate (Lateef et al. 2013) through inhibition of LPO and maintaining anti-oxidant defenses. FAR also showed a protective effect against cadmium-induced renal oxidative and genotoxic damages through inhibition of xanthine oxidase and LPO in mice (Jahangir et al. 2005). Thus, FAR can protect against HCD-induced liver injury by suppressing oxidative stress and restoring anti-oxidant defenses.

In addition to oxidative stress, HCD-fed rats showed elevated serum CRP and pro-inflammatory cytokines. Indeed, hypercholesterolemia-induced sustained ROS production can elicit stress signaling and pro-inflammatory pathways, particularly, NF- κ B signaling which is a redox-sensitive factor controlling the transcriptional regulation of IL-1 β , IL-6, and TNF- α . Here, serum levels of IL-1 β , IL-6, and TNF- α were elevated in HCD-fed rats. In addition, oxidized LDL promotes the expression of cytokines and chemokines; thereby, magnify the inflammatory response, leading to macrophage activation and more ROS generation (Lara-Guzmán et al. 2018). Within a hypercholesterolemic environment, various pathological conditions, including nonalcoholic fatty liver disease (NAFLD) and atherosclerosis can be exacerbated in the presence of systemic inflammation (Kim et al. 2014). FAR mitigated the circulating levels of pro-inflammatory mediators, demonstrating an anti-inflammatory effect. In the same context, FAR suppressed inflammation in cigarette smoke-induced lung injury- (Qamar and Sultana 2008) and acrylamide-induced neurotoxicity (Santhanasabapathy et al. 2015) in rodents.

The hepatoprotective activity of FAR could be directly connected to its anti-hypercholesterolemia efficacy. The present study explored the possible involvement of SREPB-1c, FAS, and ACC in the anti-hypercholesterolemic activity of FAR. Consistent with several previous studies (Bin-Jumah 2018; Lee et al. 2017; Ren et al. 2018), dyslipidemic rats

showed a significant increase in hepatic mRNA of SREPB-1c, FAS, and ACC. SREPB-1c is a transcription factor that regulates the expression of genes for both cholesterol and FA synthesis, including ACC and FAS, and affects the lipid accumulation induced by HFD (Horton et al. 2002). ACC and FAS have been targeted as potential intervention points for the treatment of metabolic diseases such as hyperlipidemia (Ren et al. 2018). In the present study, treatment of HCD-fed rats with FAR significantly decreased mRNA expression of liver FAS, ACC, and SREPB-1c, as well as FAS activity which can explain the observed lipid-lowering action of FAR. The suppressive effect of FAR on FAS and ACC was further investigated using molecular docking simulations. The binding affinity, hydrogen bonds, and hydrophobic interactions of FAR with ACC and FAS catalytic subunits (TE and KS) were predicted by molecular docking analysis. FAR showed both polar and hydrophobic interactions with ACC and the FAS subunits TE and KS. The TE domain is known to catalyze the liberation of the final product (palmitate) from FAS by the hydrolysis of the thioester bond in palmitoyl-S-ACP. Within the seven domains of FAS, KS is known to act as an important regulator of the produced fatty acid chain length (Cheng et al. 2008; Chirala and Wakil 2004; Witkowski et al. 2002). Polar and hydrophobic interactions play a crucial role in stabilizing geometrical structures of biological macromolecules as DNA, lipids, and proteins. Particularly, hydrogen bonding is considered to be the main factor responsible for the binding of ligands into the active sites of proteins. Consequently, they contribute to the affinity, molecular recognition, and orientation of the drug (Kubinyi 2001). The binding affinity is positively influenced by hydrophobic interactions between the lipophilic surfaces of a drug and hydrophobic zones of its binding cavity, and the total share of polar interactions to these affinities is mainly depends on desolvation energy and recently formed hydrogen bonding (Kubinyi 2001). Therefore, a perfect geometrical coincidence of a drug with the binding site is essential for a favorable protein-ligand interaction. As well, optimized geometry ligands, formation of neutral and/or charged polar bonds, and hydrophobic interactions are factors affecting the thermodynamic balance and energies of interactions (Kubinyi 2001). The agreement between docking results and the molecular and biochemical assays suggests that the affinity between FAS and ACC enzymes and FAR would provide the inhibitor with a preferable potential to exert anti-hyperlipidemia activity.

Besides the modulation of FAS and ACC, other effects of FAR contribute to its anti-dyslipidemia activity. HCD has been acknowledged to stimulate HMG-CoA reductase activation and increase its mRNA and protein expression, resulting in elevated serum LDL and hepatic cholesterol accumulation (Min et al. 2012; Shi et al. 2019). FAR has been reported to suppress and accelerate the degradation of HMG-CoA reductase (Meigs et al. 1996), thereby decreasing cholesterol

synthesis. In a rat model of hepatocarcinogenesis, FAR reduced plasma cholesterol and hepatic HMG-CoA reductase mRNA (Ong et al. 2006). Recently, Pant et al. (2019) demonstrated that FAR stimulated PPAR α -mediated induction of FAs oxidation and suppressed TG accumulation in hepatic steatosis. In HFD-fed obese KK-Ay mice, FAR ameliorated the metabolic abnormalities via PPAR α both dependent and independent pathways and suppressed SREBP-1c gene expression (Goto et al. 2011). Additionally, our results showed that FAR significantly increased the expression of LDLR which plays a crucial role in cholesterol homeostasis. LDL cholesterol uptake mediated by LDLR is an effective way of reducing circulating cholesterol (Zelcer et al. 2009), and recent studies have demonstrated elevated serum and hepatic cholesterol levels in LDLR^{-/-} mice fed a HFD (Emini Veseli et al. 2017; Sun et al. 2017). Increased phosphorylation of AMP-activated protein kinase (AMPK) is another mechanism that might be involved in the anti-hypercholesterolemic effect of FAR. AMPK plays a central role in FAs metabolism where its activation suppresses FAS and ACC and stimulates FAs β -oxidation by reducing malonyl-CoA levels (Kahn et al. 2005). The lack of data showing the effect of FAR on AMPK phosphorylation is a limitation of this study. However, FAR inhibited white adipogenesis and promoted the development of beige adipocytes in three T3-L1 cells and human adipose tissue-derived mesenchymal stem cells, respectively, through AMPK activation (Kim et al. 2017).

Conclusions

FAR attenuated hypercholesterolemia and reduced hepatic lipid accumulation and injury in HCD-fed rats. FAR reduced serum and hepatic lipids, increased LDL cholesterol clearance, attenuated oxidative stress, and inflammation. The lipid-lowering efficacy of FAR was associated with up-regulation of LDLR and down-regulation of SREBP-1c, FAS, and ACC. In addition, the results showed a good correlation between the in silico-determined binding affinity of FAR with FAS and ACC and the in vivo findings. Therefore, FAR is an effective cholesterol-lowering agent that can attenuate liver injury and the development of CVD, pending further investigations to clarify the precise mechanism of action.

Funding information The authors extend their appreciation to the Deanship of Scientific Research at Princess Nourah bint Abdulrahman University for supporting this research through the Fast-track Research Funding Program.

Compliance with ethical standards

The experimental protocol and procedures were approved by the Institutional Research Ethics Committee of Beni-Suef University (Egypt).

Consent for publication Not applicable.

Competing interests The authors declare that they have no conflict of interest.

References

- Abbas AM, Sakr HF (2013) Simvastatin and vitamin E effects on cardiac and hepatic oxidative stress in rats fed on high fat diet. *J Physiol Biochem* 69:737–750
- Al-Rasheed NM, Al-Oteibi MM, Al-Manee RZ, Al-Shareef SA, Hasan IH, Mohamad RA, Mahmoud AM (2015) Simvastatin prevents isoproterenol-induced cardiac hypertrophy through modulation of the JAK/STAT pathway. *Drug Des Devel Ther* 9:3217–3229. <https://doi.org/10.2147/DDDT.S86431> eCollection 2015
- AlSharari SD, Al-Rejaie SS, Abuhashish HM, Ahmed MM, Hafez MM (2016) Rutin attenuates hepatotoxicity in high-cholesterol-diet-fed rats. *Oxidative Med Cell Longev* 2016:5436745
- Araghi A, Golshahi H, Baghban F, Abouhosseini Tabari M (2018) Ameliorative action of farnesol on cyclophosphamide induced toxicity in mice. *Journal of Herbmol Pharmacology* 7:37–43
- Arvind A, Osganian SA, Cohen DE, Corey KE (2000) Lipid and lipoprotein metabolism in liver disease. In: Feingold KR et al (eds) *Endotext*. MDText.com, Inc., South Dartmouth
- Becke AD (1993) Density-functional thermochemistry. III. The role of exact exchange. *The Journal of Chemical Physics* 98:5648–5652
- Beutler E, Duron O, Kelly BM (1963) Improved method for the determination of blood glutathione. *J Lab Clin Med* 61:882–888
- Bin-Jumah MN (2018) Monolluma quadrangula protects against oxidative stress and modulates LDL receptor and fatty acid synthase gene expression in hypercholesterolemic rats. *Oxidative Med Cell Longev* 2018:3914384
- Bradford MM (1976) A rapid and sensitive method for the quantitation of microgram quantities of protein utilizing the principle of protein-dye binding. *Anal Biochem* 72:248–254
- Cheng F, Wang Q, Chen M, Quioco FA, Ma J (2008) Molecular docking study of the interactions between the thioesterase domain of human fatty acid synthase and its ligands. *Proteins* 70:1228–1234
- Chirala SS, Wakil SJ (2004) Structure and function of animal fatty acid synthase. *Lipids* 39:1045–1053
- Cífková R, Krajčovicová A (2015) Dyslipidemia and cardiovascular disease in women. *Curr Cardiol Rep* 17:609
- Cohen G, Dembiec D, Marcus J (1970) Measurement of catalase activity in tissue extracts. *Anal Biochem* 34:30–38
- Corbett JW, Freeman-Cook KD, Elliott R, Vajdos F, Rajamohan F, Kohls D, Marr E, Zhang H, Tong L, Tu M (2010) Discovery of small molecule isozyme non-specific inhibitors of mammalian acetyl-CoA carboxylase 1 and 2. *Bioorg Med Chem Lett* 20:2383–2388
- Csonka C, Sárközy M, Pipicz M, Dux L, Csont T (2016) Modulation of hypercholesterolemia-induced oxidative/nitrative stress in the heart. *Oxidative Med Cell Longev* 2016:3863726
- de Souza DS, de Menezes-Filho JER, Santos-Miranda A, de Jesus ICG, Neto JAS, Guatimosim S, Cruz JS, de Vasconcelos CML (2019) Calcium overload-induced arrhythmia is suppressed by farnesol in rat heart. *Eur J Pharmacol* 859:172488
- Emini Veseli B, Perrotta P, De Meyer GRA, Roth L, Van der Donck C, Martinet W, De Meyer GRY (2017) Animal models of atherosclerosis. *Eur J Pharmacol* 816:3–13
- Farrell GC, Larter CZ (2006) Nonalcoholic fatty liver disease: from steatosis to cirrhosis. *Hepatology* 43:S99–S112
- Folch J, Lees M, Sloane Stanley GH (1957) A simple method for the isolation and purification of total lipides from animal tissues. *J Biol Chem* 226:497–509

- Förstermann U (2008) Oxidative stress in vascular disease: causes, defense mechanisms and potential therapies. *Nat Rev Cardiol* 5:338
- Goodridge AG (1972) Regulation of the activity of acetyl coenzyme A carboxylase by palmitoyl coenzyme A and citrate. *J Biol Chem* 247:6946–6952
- Goto T, Kim Y-I, Funakoshi K, Teraminami A, Uemura T, Hirai S, Lee J-Y, Makishima M, Nakata R, Inoue H (2011) Farnesol, an isoprenoid, improves metabolic abnormalities in mice via both PPAR α -dependent and -independent pathways. *American Journal of Physiology-Endocrinology and Metabolism* 301:E1022–E1032
- Guido S, Joseph T (1992) Effect of chemically different calcium antagonists on lipid profile in rats fed on a high fat diet. *Indian J Exp Biol* 30:292–294
- Han Q, Yeung SC, Ip MS, Mak JC (2018) Dysregulation of cardiac lipid parameters in high-fat high-cholesterol diet-induced rat model. *Lipids Health Dis* 17:255
- Hiyoshi H, Yanagimachi M, Ito M, Yasuda N, Okada T, Ikuta H, Shinmyo D, Tanaka K, Kurusu N, Yoshida I (2003) Squalene synthase inhibitors suppress triglyceride biosynthesis through the farnesol pathway in rat hepatocytes. *J Lipid Res* 44:128–135
- Horton JD, Goldstein JL, Brown MS (2002) SREBPs: activators of the complete program of cholesterol and fatty acid synthesis in the liver. *J Clin Invest* 109:1125–1131
- Huang Y, Walker K, Hanley F, Narula J, Houser S, Tulenko T (2004) Cardiac systolic and diastolic dysfunction after a cholesterol-rich diet. *Circulation* 109:97–102
- Jahangir T, Khan TH, Prasad L, Sultana S (2005) Alleviation of free radical mediated oxidative and genotoxic effects of cadmium by farnesol in Swiss albino mice. *Redox Rep* 10:303–310
- Jung YY, Hwang ST, Sethi G, Fan L, Arfuso F, Ahn KS (2018) Potential anti-inflammatory and anti-cancer properties of farnesol. *Molecules* 23:2827
- Kahn BB, Alquier T, Carling D, Hardie DG (2005) AMP-activated protein kinase: ancient energy gauge provides clues to modern understanding of metabolism. *Cell Metab* 1:15–25
- Kim EJ, Kim B-H, Seo HS, Lee YJ, Kim HH, Son H-H, Choi MH (2014) Cholesterol-induced non-alcoholic fatty liver disease and atherosclerosis aggravated by systemic inflammation. *PLoS One* 9:e97841
- Kim H-L, Jung Y, Park J, Youn D-H, Kang J, Lim S, Lee BS, Jeong M-Y, Choe S-K, Park R (2017) Farnesol has an anti-obesity effect in high-fat diet-induced obese mice and induces the development of beige adipocytes in human adipose tissue derived-mesenchymal stem cells. *Front Pharmacol* 8:654
- Kocsis GF, Csont T, Varga-Orvos Z, Puskas LG, Murlasits Z, Ferdinandy P (2009) Expression of genes related to oxidative/nitrosative stress in mouse hearts: effect of preconditioning and cholesterol diet. *Med Sci Monit* 16:BR32–BR39
- Ku C-M, Lin J-Y (2015) Farnesol, a sesquiterpene alcohol in herbal plants, exerts anti-inflammatory and antiallergic effects on ovalbumin-sensitized and-challenged asthmatic mice. *Evid Based Complement Alternat Med* 2015:387357
- Kubinyi H (2001) Hydrogen bonding: the last mystery in drug design. 513–24
- Küçükgergin C, Aydın AF, Özdemirler-Erata G, Mehmetçik G, Koçak-Toker N, Uysal M (2010) Effect of artichoke leaf extract on hepatic and cardiac oxidative stress in rats fed on high cholesterol diet. *Biol Trace Elem Res* 135:264–274
- Lara-Guzmán OJ, Gil-Izquierdo Á, Medina S, Osorio E, Álvarez-Quintero R, Zuluaga N, Oger C, Galano J-M, Durand T, Muñoz-Durango K (2018) Oxidized LDL triggers changes in oxidative stress and inflammatory biomarkers in human macrophages. *Redox Biol* 15:1–11
- Lateef A, Rehman MU, Tahir M, Khan R, Khan AQ, Qamar W, Sultana S (2013) Farnesol protects against intratracheally instilled cigarette smoke extract-induced histological alterations and oxidative stress in prostate of wistar rats. *Toxicol Int* 20:35–42
- Lee KS, Chun SY, Kwon YS, Kim S, Nam KS (2017) Deep sea water improves hypercholesterolemia and hepatic lipid accumulation through the regulation of hepatic lipid metabolic gene expression. *Mol Med Rep* 15:2814–2822
- Livak KJ, Schmittgen TD (2001) Analysis of relative gene expression data using real-time quantitative PCR and the 2^{-Delta Delta C(T)} method. *Methods* 25:402–408
- Lu S, Archer MC (2005) Fatty acid synthase is a potential molecular target for the chemoprevention of breast cancer. *Carcinogenesis* 26:153–157
- Marklund S, Marklund G (1974) Involvement of the superoxide anion radical in the autoxidation of pyrogallol and a convenient assay for superoxide dismutase. *Eur J Biochem* 47:469–474
- McGill MR (2016) The past and present of serum aminotransferases and the future of liver injury biomarkers. *EXCLI J* 15:817–828
- Meigs TE, Roseman DS, Simoni RD (1996) Regulation of 3-hydroxy-3-methylglutaryl-coenzyme A reductase degradation by the nonsterol mevalonate metabolite farnesol in vivo. *J Biol Chem* 271:7916–7922
- Min HK, Kapoor A, Fuchs M, Mirshahi F, Zhou H, Maher J, Kellum J, Warnick R, Contos MJ, Sanyal AJ (2012) Increased hepatic synthesis and dysregulation of cholesterol metabolism is associated with the severity of nonalcoholic fatty liver disease. *Cell Metab* 15:665–674
- Muniz LB, Alves-Santos AM, Camargo F, Martins DB, Celes MRN, Naves MMV (2019) High-lard and high-cholesterol diet, but not high-lard diet, leads to metabolic disorders in a modified dyslipidemia model. *Arq Bras Cardiol* 113:896–902
- Ohkawa H, Ohishi N, Yagi K (1979) Assay for lipid peroxides in animal tissues by thiobarbituric acid reaction. *Anal Biochem* 95:351–358
- Ong TP, Heidor R, de Conti A, Dagli ML, Moreno FS (2006) Farnesol and geraniol chemopreventive activities during the initial phases of hepatocarcinogenesis involve similar actions on cell proliferation and DNA damage, but distinct actions on apoptosis, plasma cholesterol and HMGCoA reductase. *Carcinogenesis* 27:1194–1203
- Ordovas JM (2009) Genetic influences on blood lipids and cardiovascular disease risk: tools for primary prevention. *Am J Clin Nutr* 89:1509S–1517S
- Orellana-Gavalda JM, Herrero L, Malandrino MI, Paneda A, Sol Rodriguez-Pena M, Petry H, Asins G, Van Deventer S, Hegardt FG, Serra D (2011) Molecular therapy for obesity and diabetes based on a long-term increase in hepatic fatty-acid oxidation. *Hepatology* 53:821–832
- Osipov RM, Bianchi C, Feng J, Clements RT, Liu Y, Robich MP, Glazer HP, Sodha NR, Sellke FW (2009) Effect of hypercholesterolemia on myocardial necrosis and apoptosis in the setting of ischemia-reperfusion. *Circulation* 120:S22–S30
- Pant A, Rondini EA, Kocarek TA (2019) Farnesol induces fatty acid oxidation and decreases triglyceride accumulation in steatotic HepaRG cells. *Toxicol Appl Pharmacol* 365:61–70
- Pettersen EF, Goddard TD, Huang CC, Couch GS, Greenblatt DM, Meng EC, Ferrin TE (2004) UCSF chimera—a visualization system for exploratory research and analysis. *J Comput Chem* 25:1605–1612
- Qamar W, Sultana S (2008) Farnesol ameliorates massive inflammation, oxidative stress and lung injury induced by intratracheal instillation of cigarette smoke extract in rats: an initial step in lung chemoprevention. *Chem Biol Interact* 176:79–87
- Ren R, Gong J, Zhao Y, Zhuang X, Ye Y, Huang F, Lin W (2018) Sulfated polysaccharide from *Enteromorpha prolifera* suppresses SREBP-1c and ACC expression to lower serum triglycerides in high-fat diet-induced hyperlipidaemic rats. *J Funct Foods* 40:722–728
- Ross R (1992) The pathogenesis of atherosclerosis. In: Braunwald E (ed) *Heart disease: a textbook of cardiovascular medicine*. WB Saunders, Philadelphia, pp 1106–1124

- Santhanasabapathy R, Vasudevan S, Anupriya K, Pabitha R, Sudhandiran G (2015) Farnesol quells oxidative stress, reactive gliosis and inflammation during acrylamide-induced neurotoxicity: behavioral and biochemical evidence. *Neuroscience* 308:212–227
- Shi J, Li R, Liu Y, Lu H, Yu L, Zhang F (2019) Shuangyu Tiaozhi granule attenuates hypercholesterolemia through the reduction of cholesterol synthesis in rat fed a high cholesterol diet. *Biomed Res Int* 2019:4805926
- Singh UN, Kumar S, Dhakal S (2017) Study of oxidative stress in hypercholesterolemia. *Int J Con-Temp Med Res* 4:1204–1207
- Smathers RL, Galligan JJ, Stewart BJ, Petersen DR (2011) Overview of lipid peroxidation products and hepatic protein modification in alcoholic liver disease. *Chem Biol Interact* 192:107–112
- Smith S, Witkowski A, Joshi AK (2003) Structural and functional organization of the animal fatty acid synthase. *Prog. Lipid Res.* 42:289–317
- Sozen E, Ozer NK (2017) Impact of high cholesterol and endoplasmic reticulum stress on metabolic diseases: an updated mini-review. *Redox Biol* 12:456–461
- Sun YZ, Chen JF, Shen LM, Zhou J, Wang CF (2017) Anti-atherosclerotic effect of hesperidin in LDLr(−/−) mice and its possible mechanism. *Eur J Pharmacol* 815:109–117
- Szűcs G, Murlasits Z, Török S, Kocsis GF, Pálóczi J, Görbe A, Csont T, Csonka C, Ferdinandy P (2013) Cardioprotection by farnesol: role of the mevalonate pathway. *Cardiovasc Drugs Ther* 27:269–277
- Tatman D, Mo H (2002) Volatile isoprenoid constituents of fruits, vegetables and herbs cumulatively suppress the proliferation of murine B16 melanoma and human HL-60 leukemia cells. *Cancer Lett* 175:129–139
- Trott O, Olson AJ (2010) AutoDock Vina: improving the speed and accuracy of docking with a new scoring function, efficient optimization, and multithreading. *J Comput Chem* 31:455–461
- van Herpen NA, Schrauwen-Hinderling VB (2008) Lipid accumulation in non-adipose tissue and lipotoxicity. *Physiol Behav* 94:231–241
- Varga ZV, Kupai K, Szűcs G, Gáspár R, Pálóczi J, Faragó N, Zvara Á, Puskás LG, Rázga Z, Tiszlavicz L (2013) MicroRNA-25-dependent up-regulation of NADPH oxidase 4 (NOX4) mediates hypercholesterolemia-induced oxidative/nitrative stress and subsequent dysfunction in the heart. *J Mol Cell Cardiol* 62:111–121
- Voziyan PA, Goldner CM, Melnykovich G (1993) Farnesol inhibits phosphatidylcholine biosynthesis in cultured cells by decreasing cholinephosphotransferase activity. *Biochem J* 295:757–762
- Witkowski A, Joshi AK, Smith S (2002) Mechanism of the β -ketoacyl synthase reaction catalyzed by the animal fatty acid synthase. *Biochemistry* 41:10877–10887
- Xiang S, Callaghan MM, Watson KG, Tong L (2009) A different mechanism for the inhibition of the carboxyltransferase domain of acetyl-coenzyme A carboxylase by tepaloxymid. *Proc Natl Acad Sci U S A* 106:20723–20727
- Yang R-L, Shi Y-H, Hao G, Li W, Le G-W (2008) Increasing oxidative stress with progressive hyperlipidemia in human: relation between malondialdehyde and atherogenic index. *J Clin Biochem Nutr* 43:154–158
- Zelcer N, Hong C, Boyadjian R, Tontonoz P (2009) LXR regulates cholesterol uptake through idol-dependent ubiquitination of the LDL receptor. *Science (New York, N.Y.)* 325:100–104

Publisher's note Springer Nature remains neutral with regard to jurisdictional claims in published maps and institutional affiliations.